



ELSEVIER

Contents lists available at ScienceDirect

Ceramics International

journal homepage: www.elsevier.com/locate/ceramintCERAMICS
INTERNATIONAL

Anharmonicity and local noncentrosymmetric regions in BaTiO₃ pressed powder studied by the Raman line temperature dependence

A.M. Pugachev^a, I.V. Zaytseva^a, N.V. Surovtsev^a, A.S. Krylov^{b,*}^a Institute of Automation and Electrometry SB RAS, Novosibirsk, Russia, 630090^b Kirensky Institute of Physics Federal Research Center KSC SB RAS, Krasnoyarsk, Russia, 660036

ARTICLE INFO

Keywords:

BaTiO₃
 Non-hydrostatic pressure
 Raman scattering
 Anharmonicity
 Noncentrosymmetric regions

ABSTRACT

The temperature dependencies of position, width, and integral amplitude the E(TO) line near 307 cm⁻¹ in Raman spectra in barium titanate powders with different non-hydrostatic pressure and temperature treatment were studied. It was found that parameters of the E(TO) line near 307 cm⁻¹ are different in the crystal, the untreated powder, the powder treated by the non-hydrostatic pressure, and the powder annealed after the pressure treatment. The line width (FWHM) increase with temperature according to Klemens model. It indicates that the origin of the line broadening is the anharmonicity of the E(TO) phonons. The pressure treatment changes the anharmonicity of the phonon potential. It was found that the temperature dependence of the integral intensity of the E(TO) line is similar to that of the second optical harmonic signal and reflects the presence of the local polar regions. Thus, the E(TO) line in the Raman spectrum allows one to characterize the average polarity of local regions and their anharmonicity depending on non-hydrostatic pressures and thermal treatment.

1. Introduction

Non-hydrostatic pressure treatment and annealing of ferroelectric powders play a crucial role in the manufacture of electrical devices (such as capacitors, sensors, e. a.) [1]. It is well known that pressure treatment and temperature annealing not only determine the hardness and density of the resulting composite but also significantly affect its physical properties [2–5].

The effects of hydrostatic and non-hydrostatic mechanical stresses on the properties of ferroelectric powders (barium titanate (BaTiO₃), for example) are different. In the case of hydrostatic pressure, the temperature of the phase transition from tetragonal to cubic phase (further, ferroelectric phase transition) decreases [2–4]. Non-hydrostatic pressure treatment of the BaTiO₃ powders leads to an increase in temperature and width of the ferroelectric phase transition [6–10].

It was reported [6–9] that non-hydrostatic pressure treatment creates local residual mechanical stresses and corresponding electric fields in BaTiO₃ powders. The local residual mechanical stresses are assumed to be reasons for the increase of the temperature and the width of the ferroelectric phase transition that can be interpreted as the emergence of the relaxor properties in so treated samples. On the other hand, a lack of the inverse symmetry in the local polar regions can be characterized by the signal of the second optical harmonic (SHG signal) [11]. This method exploits the feature of the most perovskites that the SHG signal

is proportional to the square of the dipole moment (spontaneous polarization) [12]. In line with this, notable SHG signal in the pressed powder of barium titanate, which is notable at temperatures above the barium titanate phase transition temperature, reflects the local polar regions induced by the residual mechanical stresses after non-hydrostatic pressure treatment [8]. The magnitude of residual mechanical stresses decreases after temperature annealing [6,8].

Until now, the information about properties of the local polar regions is based on interpretations of some experiments, since well-established structural techniques cannot study these local nanometer regions. The validity of our knowledge about the properties of the local polar regions depends on the validity of the interpretations. More experimental manifestations of polar regions could help in evaluating the parameters of these regions. Here, we propose to use the capability of the E(TO) line in the Raman spectrum (near 307 cm⁻¹ in barium titanate) for uncovering the local material properties.

Previously, it was found that the position of the E(TO) line is sensitive to residual and applied mechanical stresses [8,9,18]. Hence, the Raman shift of this line can be a measure of the local mechanical stresses in barium titanate samples. On the other hand, this line is forbidden for the cubic phase and allowed for the tetragonal phase [13–15]. Therefore, its intensity reflects the portion of the polar (tetragonal-like) regions in the material. Another prospect of the Raman line application can be addressed to the description of local anharmonic

* Corresponding author.

E-mail address: shusy@iph.krasn.ru (A.S. Krylov).<https://doi.org/10.1016/j.ceramint.2020.06.024>

Received 23 May 2020; Received in revised form 1 June 2020; Accepted 2 June 2020

0272-8842/ © 2020 Elsevier Ltd and Techna Group S.r.l. All rights reserved.

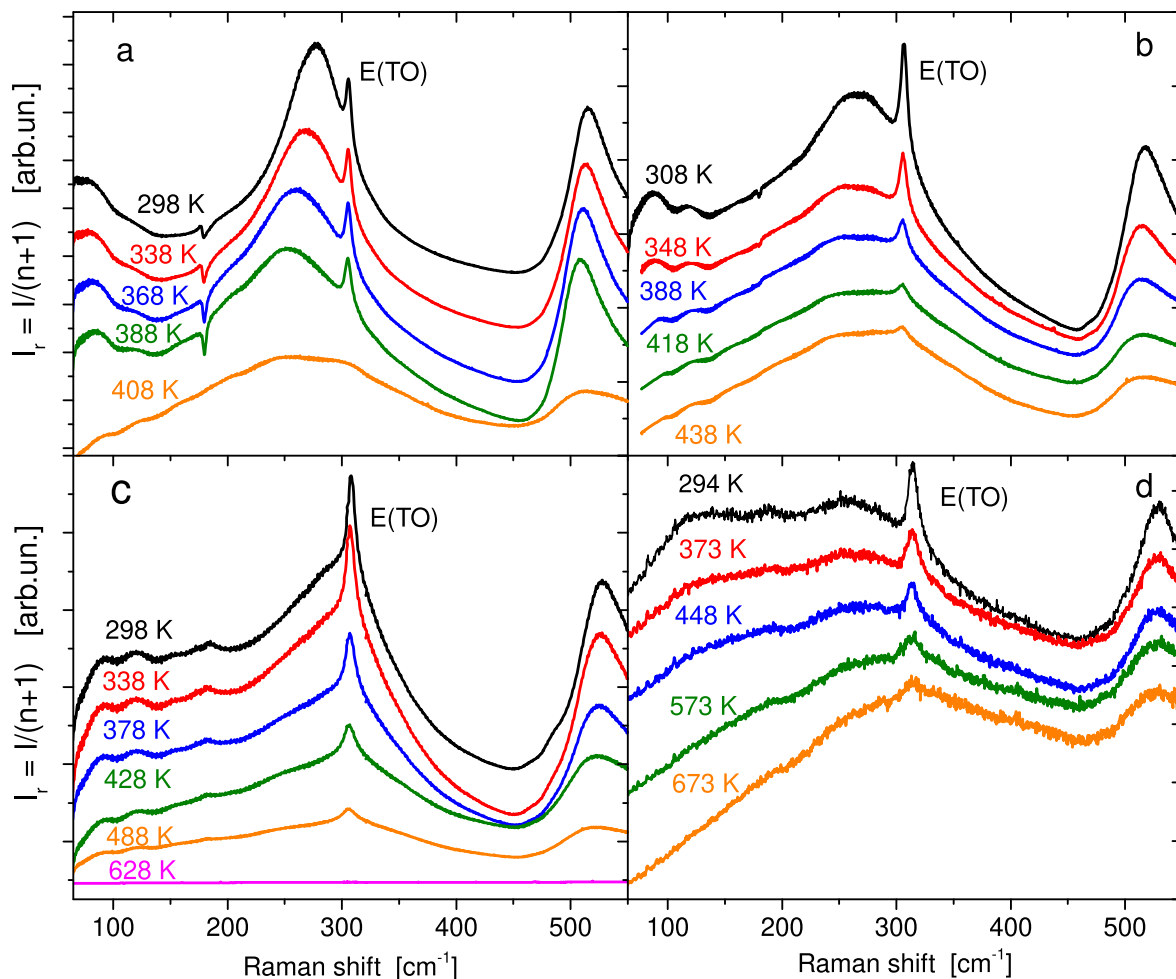


Fig. 1. Raman spectra in the susceptibility presentation for the BT1 sample (a), the BT2 sample (b), the BT3 sample (c); the BT5 sample, which is under 5 GPa pressure (d) at representative temperatures. Spectra at different temperatures are vertically shifted upward for illustrative properties.

parameters and possible distribution of the local mechanical stresses. These properties contribute to the Raman line width. The stress distribution should result in its inhomogeneous broadening, which is temperature-independent, while the properties of the materials are unchanged. The anharmonicity leads to the Lorentzian-like (homogeneous) broadening. Provided that the Raman line is narrow and homogeneously broadened, the temperature dependence of line width $\Gamma(T)$ in the cubic anharmonicity for any material can be described by the Klemens expression [16]:

$$\Gamma(T) = \gamma_0(2n(\omega_0/2, T) + 1) \quad (1)$$

Here ω_0 is line frequency, n is the Bose-Einstein distribution and γ_0 is a parameter, which proportional to the anharmonicity of the effective phonon potential. In the absence of the inhomogeneous broadening Eq. (1) usually describes well the temperature dependence of the line width. The inhomogeneous broadening results in a temperature-independent additive contribution to Eq. (1). In addition to the local stress distribution, local defects also can lead to the broadening additional to Eq. (1). This also provides a Lorentzian-like broadening, which is independent of temperature [17]. Thus, investigation of the temperature dependence of the Raman line parameters in barium titanate powders seems promising in the evaluation of the properties of local polar regions.

Here we studied the temperature dependence of the E(TO) Raman line parameters in barium titanate powders with different pressure and temperature treatment. The temperature behavior of the E(TO) Raman intensity was also compared with the SHG signal.

2. Experimental setup

2.1. Samples

A BaTiO₃ single crystal, grown by the top-seeded solution growth method, unpressed and uniaxial pressed powders were studied. The crystal was cut to (001)-oriented plate, which was polished to optical quality. A nominally pure BaTiO₃ powder was (Aldrich) with a grain size of less than 2 μm (this sample is denoted as BT2). The pressure-treated BaTiO₃ sample was prepared by applying the non-hydrostatic mechanical stresses about 10 GPa to the powder (sample BT3). Annealing, as would be expected, should decrease the residual mechanical stress after the pressure treatment. For this purpose, the pressure-treated powder was annealed for 10 h at 1200 K (sample BT4).

In order to study the powder under non-hydrostatic pressures, diamond anvils (EasyLab μScope DAC-HT(G)) were used. In this experiment, the 200 μm diameter hole was filled by the BaTiO₃ powder. No liquid transmittance media was used. The magnitude of the mechanical stresses in the sample was estimated through the shift of the Raman line from the illuminated area of the diamond anvil near the sample surface. A detailed description of this method is presented in Ref. [9]. For further presentation, we will denote the BaTiO₃ powder under non-hydrostatic pressure of 5 GPa as BT5.

2.2. Raman experiment

Back-scattering Raman spectra of the samples at ambient pressure

(BT1, BT2, BT3, BT4) were recorded with Tri Vista 777 spectrometer. Raman scattering was excited by the radiation of a 532 nm solid-state laser with a 30 mW power. In the case of the powder samples, Raman spectra were measured without polarization selection, and the polarization geometry Z(XY)Z was used for the monocrystalline sample BT1. The spectral resolution of the Raman experiment, estimated from the measurement of a neon-lamp spectrum, was about 1 cm^{-1} .

Raman experiment with the BT5 sample (under pressure) was realized with a T64000 triple spectrometer (Horiba Jobin Yvon) in back-scattering geometry. In that experiment, Raman scattering was excited by the 514.5 nm wavelength of the Ar ion laser (Spectra-Physics) with a 5 mW power.

Raman experiment was carried out in a temperature range from 300 K to 700 K with a cryostage (Linkam). All temperature experiments were made out in a zero-field cooling regime. The temperature was maintained with an accuracy of $\pm 1 \text{ K}$.

2.3. Optical second harmonic measurements

The second harmonic generation (SHG) signal was measured to characterize the average local noncentrosymmetry of material. The excitation radiation source was a pulsed laser (repetition rate is 1 kHz, the wavelength is 1064 nm, the pulse duration is 0.6 ns, and the average power is 80 mW). The SHG signal was selected from the back-scattering light by a monochromator and detected by a photomultiplier. The experimental setup is described in detail in Ref. [11]. The Linkam cryostage was used to change the temperature.

3. Results and discussion

Raman spectra at representative temperatures are shown in Fig. 1 for the samples BT1, BT2, BT3, BT5. Raman spectra from the sample BT4 are similar to the spectra of the BT2 sample and are not shown in Fig. 1 to eliminate the trivial temperature dependence for inelastic scattering from phonons. The Raman spectra are shown in Fig. 1 in the susceptibility presentation, corresponding to the Stokes Raman signal divided by $(n(\omega, T) + 1)$. Here, $n(\omega, T)$ is the Bose-Einstein distribution.

Narrow Raman line near 307 cm^{-1} , which is seen in the spectra of Fig. 1, corresponds to the scattering from the E(TO) phonons. Wider bands with maxima near 270 and 510 cm^{-1} are from phonons of the A1 symmetry [18]. In the present work, we want to reveal the effects of local properties on the Raman line. For this purpose, the narrow line 307 cm^{-1} looks prospective.

Since the E(TO) line is superposed with the broad band, the contribution from the broad band was subtracted from the Raman spectrum. For the subtraction, the broad band contribution was described

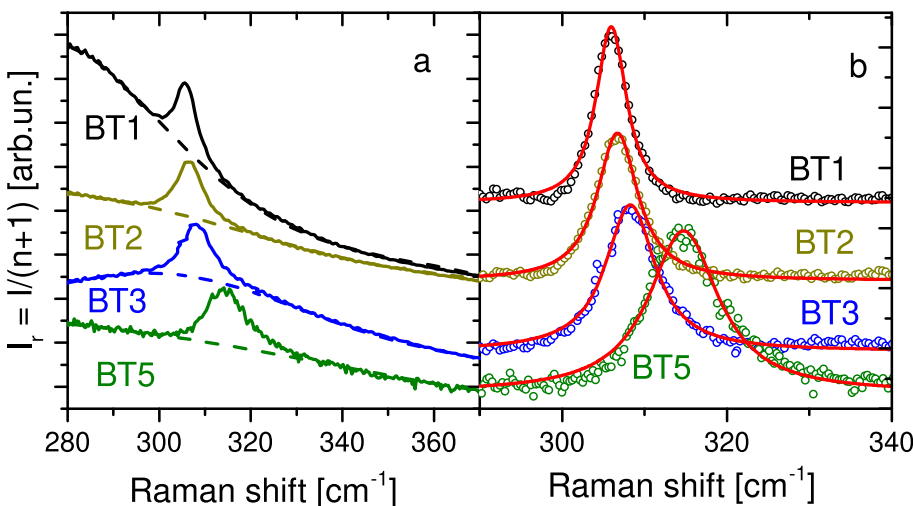


Fig. 2. (a) Room temperature Raman spectra near E(TO) peak for the BT1, BT2, BT3, and BT5 samples. Dash lines correspond to the interpolation of the broad band contribution. (b) The E(TO) peak after correction to the wide band contribution (circles). Lines are the Voigt contour fits of the narrow Raman lines near 307 cm^{-1} with subtracted baselines. Curves are vertically shifted upward for illustrative properties.

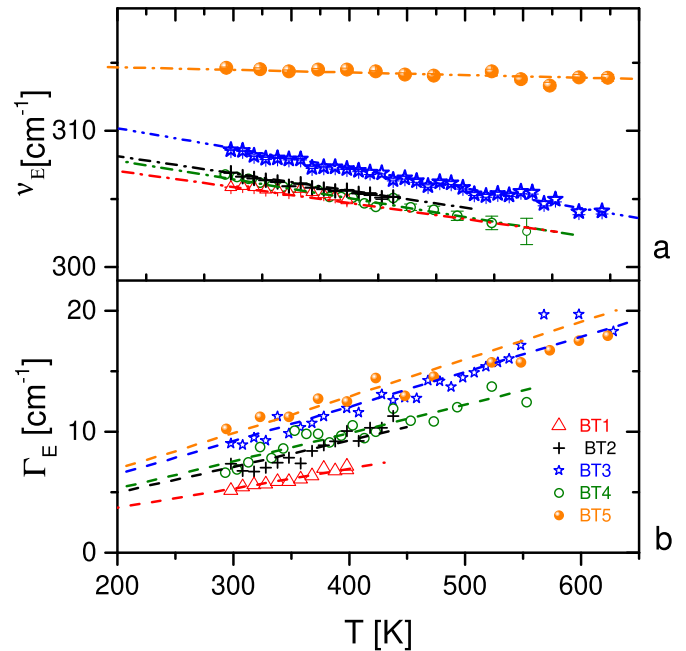


Fig. 3. Temperature dependences of $\nu_E(T)$ (a) and $\Gamma_E(T)$ (b) for the BT1 (open triangles), BT2 (crosses), BT3 (open stars), BT4 (open circles), BT5 (filled circles). Dashed-dot lines in (a) are linear fits of $\nu_E(T)$. Dashed lines in (b) are fits by Eq. (1).

by a polynomial, as shown in Fig. 2a. The 307 cm^{-1} peaks in the so-corrected Raman spectra (Fig. 2b) were fitted by the Voigt function, where the Gaussian component was fixed to the spectral resolution (1 cm^{-1}). Examples of these fits are shown in Fig. 2b.

The Voigt fits provided of the peak position ν_E in wavenumbers and its FWHM Γ_E (Lorentzian's part of the fit). The temperature dependences of the peak position ν_E and Γ_E in all samples under study are shown in Fig. 3. The temperature dependences of $\nu_E(T)$ (Fig. 3a) of the samples under ambient pressure demonstrate a moderate decrease with temperature increase. The sample under the 5 GPa pressure (BT5) shows almost temperature independent $\nu_E(T)$.

It is worth noting that $\Gamma_E(T)$ increases with temperature (Fig. 3b). Qualitatively this increase is similar for all samples, including the sample under pressure (BT5). The phonon lifetime shortening causes the peak broadening due to multiphonon interaction. Three-phonon anharmonic interaction predicts the behavior of Eq. (1). In the case of enough high temperatures, when $T \gg h\nu_E/2ck_B$ (c is the speed of

Table 1

Description of the sample		ν_E [cm ⁻¹]	γ_0 [cm ⁻¹]
BT1	BaTiO ₃ crystal	309.5	1.9
BT2	unpressed powder	311.0	2.5
BT3	powder treated by non-hydrostatic pressure 10 GPa	313.0	3.3
BT4	powder treated by non-hydrostatic pressure 10 GPa and annealed during 10 h at 1200 K	310.5	2.7
BT5	powder placed in EasyLab μ Scope DAC-HT(G) under pressure 5 GPa	317.5	3.6

light), Eq. (1) corresponds to a linear temperature behavior

$$\Gamma_E(T) = \frac{2\gamma_0 ck_B}{\nu_E h} T + \gamma_0 \quad (2)$$

Note, slope and constant of the linear function are related. It is worth also noting that Eq. (2) can be applied for any material with homogeneously broadened Raman line: it was used for the description of the temperature dependence of the width of the narrow Raman line in diamond with nitrogen impurities [17].

Experimental $\Gamma_E(T)$ was fitted by Eq. (1) with ν_E from the experiment (Fig. 3a). For this purpose, the experimental points were described by the straight lines, as shown in Fig. 3a by the dashed lines. The fits $\Gamma_E(T)$ are shown in Fig. 3b. It is seen that the temperature interval considered corresponds to the case of Eq. (2) ($T > h\nu_E/2ck_B$). Nontrivial relation between the slope and constant predicted by Eq. (2) is well fulfilled. This confirms that the three-phonon anharmonicity is responsible for the temperature dependence $\Gamma_E(T)$. Parameters of the fits are given in Table 1.

A fair description of $\Gamma_E(T)$ by the Klemens formula Eq. (1) indicates that the origin of the line broadening is the anharmonicity of the E(TO) phonons. The line broadening depends on the applied or residual mechanical stresses, as it is seen for the BT3 and BT5 sample data. A change in the anharmonicity parameter can be due to the electron-phonon interaction, which, in particular, leads to the appearance of line asymmetry [19–21]. In our case, the studied lines are symmetrical. This result evidences that the defects created by the pressure treatment change the anharmonicity parameter. Possible effects of these defects on the inhomogeneous broadening in the spirit of [17] or in the spatial distribution of the phonon frequencies are not manifested in $\Gamma_E(T)$ (Fig. 3b), since in this case, a temperature-independent term should appear in addition to Eq. (1). Hence, the main effect of the pressure treatment for phonons is related to the change of the anharmonicity.

The manifestation of the E(TO) peak in the Raman spectrum is an “indicator” of the tetragonal phase [12,13,16,17], it is forbidden in the cubic phase. Hence, it can be expected that the E(TO) peak intensity in Raman spectrum A_E reflects the average local nonsymmetry of material. On the other hand, the SHG signal should also reflect the nonsymmetry of local polar regions. In this case, the interrelation between the E(TO) peak intensity and the SHG signal is expected.

Parameter A_E was found from the experimental Raman spectra, which were normalized by the integral over the Raman spectrum in a frequency range from 80 to 550 cm⁻¹. To avoid the effects of the pressure-induced changes in polarizability, we considered the temperature dependences of A_E data scaled to its low-temperature limit. The temperature dependences of $A_E(T)$ found in our experiment are shown in Fig. 4a for the samples. Fig. 4a demonstrates that pressure treatment of powder has significant effects on $A_E(T)$, where the presence of local nonsymmetry is observed at temperatures significantly above T_m .

In the case of local uncorrelated dipoles, the square root from the experimental SHG signal $I_{2\omega}^{0.5}$ is proportional to an average local dipole moment (spontaneous polarization) [13]. Temperature dependences $I_{2\omega}^{0.5}(T)$ were scaled to their low-temperature value. Dependences $I_{2\omega}^{0.5}(T)$ are shown in Fig. 4b. In this figure, a logarithmic scale is used to

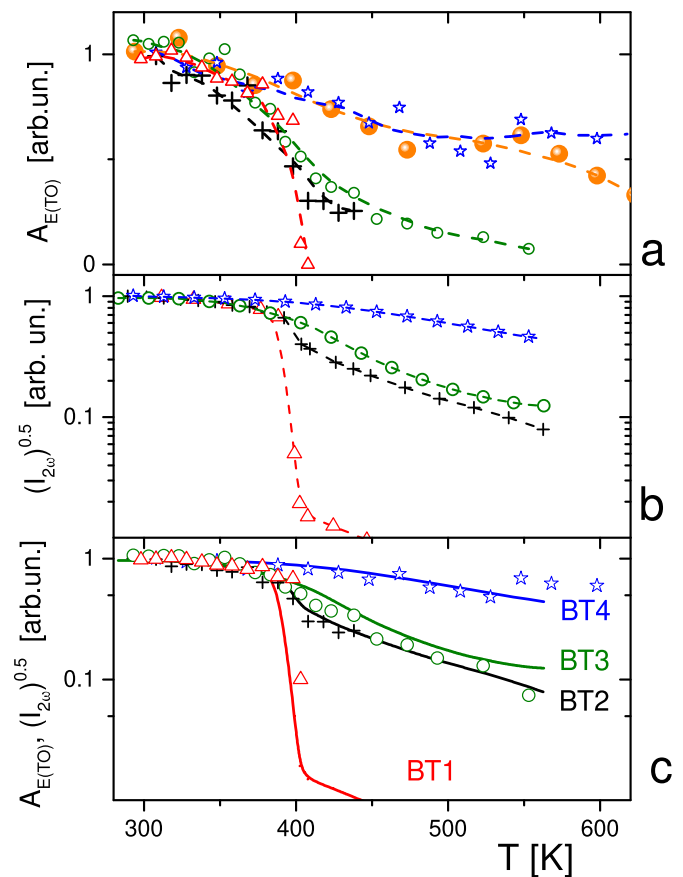


Fig. 4. Temperature dependences of Raman intensity of the E(TO) line (a), the square root of the SHG signal (b) for BT1 samples (open triangles), BT2 (crosses), BT3 (open stars), BT4 (open circles), BT5 (filled circles) samples. Lines in (a) and (b) are smooth curves connecting experimental points. Part (c) represents the comparison of $A_E(T)$ (lines, which correspond to lines in part (a)) and $I_{2\omega}^{0.5}(T)$ (symbols, in the same notation as in parts above).

visualize the wide diapason of the values. In the crystal (BT1 sample), the SHG values reflect a typical behavior for the first-order phase transition, whereas the phase transition is broadened in the powder (BT2 sample). In pressure-treated powders (BT3 sample), the phase transition to the cubic phase is not recognizable up to 650 K. Temperature annealing at 1200 K removes residual mechanical stresses. In this case, the BT4 sample and the untreated powder (BT2 sample), despite the difference in density and hardness, demonstrate approximately the same dependences $I_{2\omega}^{0.5}(T)$, corresponding to the similar behaviors of total dipole moment.

The phase transition to the cubic phase occurs in BaTiO₃ at room temperature if hydrostatic pressure exceeds 2 GPa [4,5,13]. Earlier studies of the Raman spectra in crystals and ceramics of barium titanate also show the presence of an E(TO) peak in the tetragonal phase at high non-hydrostatic pressures (above 5 GPa) [22,23]. Similar results were also obtained for SHG [6,8,11,24–26]. These facts indicate the presence of significant disorder in the high-pressure cubic phase.

The similarity between curves in Fig. 4a and b are seen. The comparison between the temperature dependences of $A_E(T)$ and $I_{2\omega}^{0.5}(T)$ is made in Fig. 4c. In this figure, the temperature dependences $I_{2\omega}^{0.5}(T)$ are shown by lines connecting smoothed experimental points (they are also present in Fig. 4a for illustration). Fig. 4c demonstrates the good agreement between $A_E(T)$ and $I_{2\omega}^{0.5}(T)$ for all samples under study. These results prove that $A_E(T)$ describes the temperature dependence of the average dipole moment in the BaTiO₃ samples, which originated from the local polar regions.

4. Conclusions

Raman spectra in BaTiO₃ crystal, powder, and powders treated by non-hydrostatic pressure were investigated. It was found that the position, width, and integral amplitude of the E(TO) line near 307 cm⁻¹ are different in the crystal, the untreated powder, the powder treated by the non-hydrostatic pressure, and the powder annealed after the pressure treatment. The temperature dependences of the line width (FWHM) prove that the pressure treatment changes the anharmonicity of the phonon potential. The temperature dependence of the integral Raman intensity of the E(TO) line demonstrates that noncentrosymmetric regions present in powders at a temperature much above the ferroelectric phase transition. Pressure treatment increases the non-symmetry of BaTiO₃ powder at high temperatures. Comparison with the temperature dependence of the SHG signal, which reflects the non-symmetry of the local polar regions, reveals that the Raman E(TO) line intensity also reflects the presence of the local polar regions. Annealing of the treated powder decreases this nonsymmetry. A comparison with Raman of the BaTiO₃ powder under pressure indicates the similarity with the behavior of the pressure-treated powder.

Thus, the non-hydrostatic pressure treatment of the BaTiO₃ powder increases the average polarity of local regions and their anharmonicity, and this can be characterized by the Raman line of the E(TO) phonon.

Declaration of competing interest

The authors declare that they have no known competing financial interests or personal relationships that could have appeared to influence the work reported in this paper.

Acknowledgement

The reported study was funded by RFBR, according to the research project No. 18-02-00399 and 19-42-543-016, Government of Novosibirsk region No. 19-42-543-016 and State assignment No AAAA-A17-117052410033-9. The experiments were performed in the multiple-access center “High-Resolution Spectroscopy of Gases and Condensed Matter” in IA&E SB RAS (Novosibirsk, Russia) and Center for Common Use of the Krasnoyarsk Scientific Center, SB RAS (Krasnoyarsk, Russia).

References

- [1] K. Okadzaki, *Technology of Ceramic Dielectrics (Russian Translation)*, Energiya, Moscow, 1976.
- [2] G.A. Samar, Pressure and temperature dependences of the dielectric properties of the perovskites BaTiO₃ and SrTiO₃, *Phys. Rev.* 151 (1996) 378–386.
- [3] W.J. Merz, The effect of hydrostatic pressure on the curie point of barium titanate single crystals, *Phys. Rev.* 77 (1950) 52–54.
- [4] Iniguez Jorge, David Vanderbilt, First-principles study of the temperature-pressure phase diagram of BaTiO₃, *Phys. Rev. Lett.* 89 (2002) 115503.
- [5] S.A. Hayward, E.K.H. Salje, The pressure-temperature phase diagram of BaTiO₃: a macroscopic description of the low-temperature behaviour, *J. Phys. Condens. Matter* 14 (2002) L599–L604.
- [6] A.M. Pugachev, I.V. Zaytseva, V.I. Kovalevskii, V.K. Malinovsky, N.V. Surovtsev, Yu M. Borzdov, I.P. Raevski, S.I. Raevskaya, M.A. Malitskaya, Local residual stresses in pressure-treated barium titanate powders probed by second harmonic generation, *Ferroelectrics* 501 (2016) 9–14.
- [7] A.M. Pugachev, I.V. Zaytseva, A.S. Krylov, V.K. Malinovsky, N.V. Surovtsev, Yu M. Borzdov, V. Kovalevsky, Uniaxial mechanical stresses and their influence on the parameters of the ferroelectric phase transition in pressure-treated barium titanate, *Ferroelectrics* 508 (2017) 161–166.
- [8] A.M. Pugachev, V.I. Kovalevsky, V.K. Malinovsky, Yu M. Borzdov, N.V. Surovtsev, Relaxor-like features in pressure-treated barium titanate powder, *Appl. Phys. Lett.* 107 (2015) 102902.
- [9] I.V. Zaytseva, A.M. Pugachev, K.A. Okotrub, N.V. Surovtsev, S.L. Mikerin, A.S. Krylov, Residual mechanical stresses in pressure treated BaTiO₃ powder, *Ceram. Int.* 45 (2019) 12455–12460.
- [10] E.I. Bondarenko, Z.V. Bondarenko, M.V. Lomakov, I.P. Raevskii, Effects of residual mechanical stress on phase transition in hot-pressed ferroelectric ceramics, *Sov. Phys. Tech. Phys.* 30 (1985) 582–583.
- [11] M. Pugachev, V.I. Kovalevskii, N.V. Surovtsev, S. Kojima, S.A. Prosandeev, I.P. Raevski, S.I. Raevskaya, *Phys. Rev. Lett.* 108 (2012) 247601.
- [12] M.E. Lines, A.M. Glass, *Principles and Applications of Ferroelectrics and Related Materials*, Mir, Moscow, 1981, Oxford University Press, Oxford, 1977, p. 736.
- [13] Uma D. Venkateswaran, Vaman M. Naik, Ratna Naik, High-pressure Raman studies of polycrystalline BaTiO₃, *Phys. Rev. B* 58 (1998) 14256.
- [14] M. Di Domenico, S.H. Wemple, S.P.S. Porto, R.P. Bauman, Raman spectrum of single-domain BaTiO, *Phys. Rev.* 174 (1968) 522.
- [15] Yu I. Yuzuk, Raman scattering spectra of ceramics, films, and superlattices of ferroelectric perovskites: a review, *Phys. Solid State* 54 (2012) 1026–1059.
- [16] P.G. Klemens, Anharmonic decay of optical phonons, *Phys. Rev.* 148 (1966) 845.
- [17] Nikolay V. Surovtsev, Igor N. Kupriyanov, Effect of nitrogen impurities on the Raman line width in diamond, *Revist. Cryst.* 7 (2017) 239, <https://doi.org/10.3390/cryst7080239>.
- [18] A. Pinczuk, W. Taylor, E. Burstein, I. Lefkowitz, The Raman spectrum of BaTiO₃, *Solid State Commun.* 5 (1967) 429–433.
- [19] Manushree Tanwar, Devesh K. Pathak, Anjali Chaudhary, Priyanka Yogi, Shailendra K. Saxena, Rajesh Kumar, Mapping longitudinal inhomogeneity in nanostructures using cross-sectional spatial Raman imaging, *J. Phys. Chem. C* 124 (2020) 6467–6471.
- [20] Priyanka Yogi, Suryakant Mishra, Shailendra K. Saxena, Vivek Kumar, Rajesh Kumar, Fano scattering: manifestation of acoustic phonons at nanoscale, *J. Phys. Chem. Lett.* 7 (24) (2016) 5291–5296.
- [21] Priyanka Yogi, Deepika Poonia, Suryakant Mishra, Shailendra K. Saxena, Swarup Roy, Vivek Kumar, Pankaj R. Sagdeo, Rajesh Kumar, Spectral anomaly in Raman scattering from p-type silicon nanowires, *J. Phys. Chem. C* 121 (2017) 5372–5378.
- [22] I.V. Zaytseva, A.M. Pugachev, N.V. Surovtsev, A.S. Krylov, Features of Raman spectra in barium titanate pressed powder, SPM-2019-RCWDFM Joint International Conference, IOP Conf. Ser. Mater. Sci. Eng. 699 (2019) 012058.
- [23] W. Zhang, L. Chen, C. Jin, X. Deng, X. Wang, L. Li, High pressure Raman studies of dense nanocrystalline BaTiO₃ ceramic, *J. Electroceram.* 21 (2008) 859–862.
- [24] J.P. Dougherty, S.K. Kurtz, A second harmonic analyzer for the detection of non-centrosymmetry, *J. Appl. Cryst.* 9 (1976) 145.
- [25] G.V. Liberts, V. Ya Fritsberg, SHG investigations in the paraelectric phase of perovskite type ferroelectrics, *Phys. Status Solidi* 67 (1981) K81.
- [26] G.R. Fox, J.K. Jamamoto, D.V. Miller, L.E. Cross, S.K. Kurtz, Thermal hysteresis of optical second harmonic in paraelectric BaTiO₃, *Mater. Lett.* 9 (1990) 284.